

# Chapter 2

## Theory of Compressible Fluid Flow

### 2.1 One-Dimensional Theory of Compressible Fluid Flow

#### 2.1.1 Equation of State and the First Principal Law

The thermodynamic properties of a homogeneous and isotropic medium are fully characterized by the three quantities *temperature*  $T$  (K), *pressure*  $p$  (Pa), and *density*  $\rho$  (kg/m<sup>3</sup>) which are called the state variables. About the microscopic structure of the medium the only necessary assumptions are that the particles that constitute the medium are small enough to justify the assumption of homogeneity and that for any given set of  $T, p, \rho$  the composition of the medium is fixed. This includes, for example, mixtures of gases or air that contains a certain amount of water in the form of small droplets.

The quantities  $T, p, \rho$  depend on each other, their relation is given by the equation of state of that medium.

$$p = p(\rho, T) \quad (2.1)$$

Additional state variables can and will be defined and used but—together with the equation of state—always two of them are enough to characterize the state of the medium. In the case of a perfect gas the equation of state has the well-known form

$$p = \frac{R}{m} \rho T \quad (2.2)$$

where  $R$  is the gas constant that is given by  $R = k_B N_A = 8314.46 \text{ J/(kg K)}$ . Here  $k_B$  is the Boltzmann constant and  $N_A$  the Avogadro constant.  $m$  is the atomic (molecular) weight of the medium.

By introducing now the general physical principle of energy conservation one immediately arrives at the first principle law of thermodynamics that essentially states the conservation of energy in its transformation from heat to mechanical

energy and vice versa. The quantity that measures the energy content of a medium is the inner energy  $e$  and is a state variable on its own. Hence, it only depends on two other state variables, for example,  $e = e(p, \rho)$  which again represents an equation of state. In the case of the perfect gas, the inner energy only depends on the temperature  $e = e(T)$ . This inner energy is constant as long as the gas is not doing any work thereby converting a part of its inner energy into mechanical energy. This does not entirely exclude changes of the volume of the gas as can be seen in the following case: a perfectly isolated vessel that is separated in two compartments by a removable wall with one compartment being filled with a gas of a certain pressure and temperature. By removing the wall, the gas will now expand and fill the entire vessel. Since there is now energy (heat) transport through the vessel walls, the inner energy must be conserved which means for a perfect gas that after the expansion is completed the gas will still have the initial temperature. This is a so-called irreversible adiabatic expansion because it is impossible to reach the initial state without energy transfer to the gas. If the wall is now replaced by a slowly moving piston, the situation is different: the gas exerts a force on the piston corresponding to its pressure times the piston surface. By moving the piston a distance  $ds$ , the work  $pAd s$  is done. Since  $Ad s$  is equal to the change of the volume of the gas, the amount of work done is given by  $pdV = pd(1/\rho)$ . If heat transport to the medium  $dq$  is now considered, then the law of energy conservation takes on the form:

$$dq = de + pd(1/\rho) \quad (2.3)$$

Here the amount of heat  $q$  is measured in joule per kg. This equation is called the first principle law of thermodynamics. With the enthalpy  $i$  being defined as

$$i = e + p/\rho \quad (2.4)$$

it can be written as

$$dq = di - 1/\rho dp \quad (2.5)$$

Heat can be transferred to a medium in different ways, the two most easily realizable methods are maintaining the volume and hence the density constant and keeping the pressure constant. By measuring the amount of energy needed to raise the temperature of the medium by 1 K one arrives at the definition of the specific heats  $c_p$  and  $c_v$ . They are defined as

$$c_v = \left( \frac{\partial q}{\partial T} \right)_v = \left( \frac{\partial e}{\partial T} \right)_v \quad (2.6)$$

for constant volume and as

$$c_p = \left( \frac{\partial q}{\partial T} \right)_p = \left( \frac{\partial i}{\partial T} \right)_p \quad (2.7)$$

for constant pressure. The ratio between the specific heat is ascribed the symbol  $\kappa$  and is defined as

$$\kappa = c_p/c_v \quad \kappa = \frac{2+f}{f} \quad (2.8)$$

The equation to the right gives a connection to the kinetic theory of gases with  $f$  corresponding to the number of degrees of freedom of the molecules constituting the medium. Possible values for  $f$  are therefore three for atoms, five for molecules containing two atoms, and seven for molecules containing three or more atoms.

For the perfect gas, one obtains for the specific heats

$$de = c_v dT \quad (2.9)$$

and

$$di = c_p dT \quad (2.10)$$

Substituting this into (2.4) and using (2.2) we get

$$R/m = c_p - c_v \quad (2.11)$$

With the additional assumption that a medium not only behaves like a perfect gas but also has constant specific heats  $c_p$  and  $c_v$  for all temperatures from (2.9) and (2.10) we get

$$e = c_v T + \text{const} \quad (2.12)$$

and

$$i = c_p T + \text{const} \quad (2.13)$$

### 2.1.2 Changes of State

A medium can change its thermodynamic state in many different ways and it makes sense to distinguish between several special cases of such processes. In general, this is done by categorizing by state variables that remain constant during the whole process. This immediately gives the three processes that keep one of the state variables in the equation of state (2.1) constant, namely the isothermal, the isobaric, and the isochoric process. For many gas flows, however, another process is of interest: it is called isentropic process, is equivalent to a reversible adiabatic process, and is defined by the absence of heat flux across the boundaries of the system and also within the medium. This means that each small volume  $dV$  of the medium is in pressure-equilibrium with its surroundings and does not receive or lose any heat energy. The validity of this assumption will be discussed later.

To justify the name *isentropic*, the variable of state called entropy  $s$  is first introduced. It is defined by

$$ds = \frac{dq}{T} = \frac{de + pd(1/\rho)}{T} = \frac{di - 1/\rho dp}{T} \quad (2.14)$$

For the perfect gas with constant specific heat this can be integrated immediately and gives:

$$s_2 - s_1 = c_v \ln \frac{T_2}{T_1} - (c_p - c_v) \ln \frac{\rho_2}{\rho_1} = c_p \ln \frac{T_2}{T_1} - (c_p - c_v) \ln \frac{p_2}{p_1} = c_v \ln \frac{p_2}{p_1} - c_p \ln \frac{\rho_2}{\rho_1} \quad (2.15)$$

Here the subscripts 1 and 2 refer to the initial and the final state of the medium, respectively. For the isentropic process  $ds$  is equal to zero, Eq. 2.14 shows that this is equal to constant heat energy  $dq$  and for  $ds = 0$ :

$$0 = de + pd\left(\frac{1}{\rho}\right) \quad (2.16)$$

$$0 = di - \frac{1}{\rho} dp \quad (2.17)$$

with (2.9) and (2.11) this can be integrated and yields the following equations for the isentropic change of state from state 1 to state 2:

$$\frac{\rho_2}{\rho_1} = \left(\frac{T_2}{T_1}\right)^{\frac{1}{\kappa-1}} \quad (2.18)$$

$$\frac{p_2}{p_1} = \left(\frac{T_2}{T_1}\right)^{\frac{\kappa}{\kappa-1}} \quad (2.19)$$

$$\frac{p_2}{p_1} = \left(\frac{\rho_2}{\rho_1}\right)^{\kappa} \quad (2.20)$$

The concept of entropy also leads to the formulation of the second principal law of thermodynamics that states that the entropy of an isolated system can only increase or stay constant.

### 2.1.3 Compressible Gas Flow in 1D: Perturbations and Shocks

In the following, basic equations will be derived that describe the change of state between two spatially separated points (1) and (2) within a flowing compressible medium. In order to treat flowing media besides two thermodynamic state variables one more variable is needed to fully describe the system. This additional

variable is the flow velocity  $w$  which is a scalar quantity in the one-dimensional analysis. The three equations needed to determine these variables are the continuity Eq. 2.21, the equation of motion (2.22), and the energy conservation (2.23) given here for the case of no external forces and steady state.

$$\rho_1 w_1 = \rho_2 w_2 \quad (2.21)$$

$$p_1 + \rho_1 w_1^2 = p_2 + \rho_2 w_2^2 \quad (2.22)$$

$$\frac{w_1^2}{2} + i_1 = \frac{w_2^2}{2} + i_2 \quad (2.23)$$

They describe the flow of a medium along a stream line connecting the start-point labelled by index (1), and the endpoint labelled by index (2). Since no assumption is necessary about the actual distance between the two points, the following derivation is equally valid for continuous variation between over extended distances and for discontinuous variations in the limit of zero distance. As it turns out, both cases exist in nature, the first one representing smooth gas flow without discontinuities in the state variables and the second one describing discontinuous shocks naturally emerging in supersonic flows. Both cases will be treated in the following.

Substituting now  $i_2 = i_0 = i(T = 0K)$  and  $w_1 = 0$  in Eq. 2.23 gives the interesting result that a gas that was initially at rest and then expands freely thereby converting its whole enthalpy into kinetic energy will obtain a maximum final velocity of

$$w_{2,max} = \sqrt{2(i_1 - i_0)} \quad (2.24)$$

or, assuming a perfect gas with constant specific heat:

$$w_{2,max} = \sqrt{2c_p T} \quad (2.25)$$

For nitrogen at room temperature this evaluates to 790 m/s, for Helium to 1,765 m/s. In order to obtain one equation that describes the entire process, first the continuity Eq. 2.21 is used to write the equation of motion (2.22) as

$$\frac{w_2^2}{2} - \frac{w_1^2}{2} + \frac{1}{2} \left( \frac{1}{\rho_1} + \frac{1}{\rho_2} \right) (p_2 - p_1) = 0 \quad (2.26)$$

and then by substituting (2.23) for the velocities  $w_1$  and  $w_2$  finally equation

$$i_2 - i_1 = \frac{1}{2} \left( \frac{1}{\rho_1} + \frac{1}{\rho_2} \right) (p_2 - p_1) \quad (2.27)$$

is obtained. It describes a change of state along the so-called Rankine–Hugoniot curve. If the enthalpy  $i$  of the medium as a function  $i(p, \rho)$  is known, then this formula describes the relation between density and pressure for the flowing medium. Another important relation, namely the one for the speed of sound, can be obtained by substituting (2.21) into (2.22), thereby eliminating  $w_2$ :

$$w_1 = \sqrt{\frac{\rho_2 p_2 - p_1}{\rho_1 \rho_2 - \rho_1}} \quad (2.28)$$

In the limit  $\Delta p \rightarrow 0$  and  $\Delta \rho \rightarrow 0$  this gives the partial derivative

$$w = \sqrt{\left(\frac{\partial p}{\partial \rho}\right)_H} \quad (2.29)$$

where the subscript H denotes the derivative to be taken along the Rankine–Hugoniot curve. This is not the speed of sound but the speed of propagation of perturbation of arbitrary strength. In fact, it will be shown below that this speed can be substantially larger than the sound-speed. For *small* pressure and density changes, however, it can be shown [1] that the change of state according to Rankine–Hugoniot and the isentropic change of state coincide up to to the second order. Therefore, for small perturbations, the well-known formula for the speed of sound is obtained.

$$w = c = \sqrt{\left(\frac{\partial p}{\partial \rho}\right)_s} \quad (2.30)$$

Here  $c$  is introduced for the sound speed and the index  $s$  indicates that the derivative has to be taken while keeping the entropy  $s$  constant. This derivation immediately shows the area of applicability of this formula: It describes the propagation speed of *small* perturbations in a compressible medium. For the perfect gas (2.30) evaluates to

$$c = \sqrt{\kappa \frac{R}{m} T} = \sqrt{c_p (\kappa - 1) T} \quad (2.31)$$

yielding at temperature of 300 K for Air 347 m/s and for Helium 1.02 km/s.

As detailed below, strong distortions are able to propagate at speeds (much) larger than the speed of sound. For the perfect gas,  $i(p, \rho)$  can be obtained by substituting (2.11) and (2.8) into (2.2) and the result into (2.13):

$$i(p, \rho) = \frac{\kappa}{\kappa - 1} \frac{p}{\rho} \quad (2.32)$$

This allows to obtain from (2.27) an (implicit) relation between  $p$  and  $\rho$  along the Rankine–Hugoniot curve:

$$\frac{p_2 - p_1}{\rho_2 - \rho_1} = \kappa \frac{p_2 + p_1}{\rho_2 + \rho_1} \quad (2.33)$$

Figure 2.1a shows a plot of the density-ratio over the pressure ratio for the Rankine–Hugoniot case and the isentropic case. As can be seen, the value of the Rankine–Hugoniot curve tends asymptotically towards  $(\kappa + 1)/(\kappa - 1)$  whereas the isentropic one increases with  $(p_2/p_1)^{1/\kappa}$ . As mentioned above, the

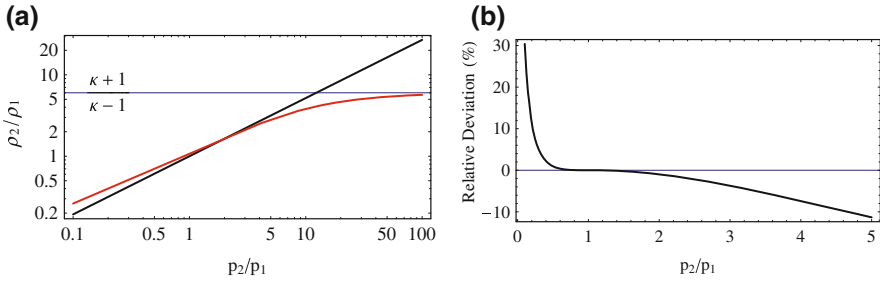


**Fig. 2.1** Comparison between Rankine–Hugoniot and isentropic process for  $N_2$  (perfect gas) with constant specific heat. **a** Rankine–Hugoniot (red) and isentropic curve (black). **b** Relative difference between Rankine–Hugoniot and isentropic curve

Rankine–Hugoniot curve is the correct one for compressions with large pressure ratios. For pressure ratios close to one the two curves coincide, Fig. 2.1b shows the relative difference between the two curves. Finally, for pressure ratios smaller than one, thus corresponding to expansion, all curves with a density-ratio larger than the one of the isentropic curve are prohibited by the second principal law because they would imply a decrease of entropy during the expansion. Since no assumption has been made so far concerning the distance between points (1) and (2), in principle the above results are applicable for large distances as well as for the limit of the distance going to zero. The latter one does actually occur in nature in the form of compression shocks in supersonic flows. Since the pressure jump in such a shock is usually comparable to the static pressure of the gas, it must always be considered a strong distortion. This implies that the Rankine–Hugoniot equations have to be used for the description of supersonic compression shocks.

Such shocks naturally occur always when a supersonic flow encounters some sort of obstacle in its path. Thinking first of a subsonic flow, it is clear that the flow will be influenced downstream *and* upstream therefore leading to a smooth adaptation of the flow that starts already well ahead of the position of the obstacle. This leads to a smooth transition from the unperturbed flow field far upstream to the deformed flow field close to the object. In the case of a supersonic flow, this is impossible because *smooth* upstream adaptation is equivalent to the upstream propagation of small perturbations that cause the gradual flow field deformation as the gas streams in from the unperturbed far field and gets closer to the obstacle. Only a *strong* perturbation in the form of a discontinuous shock is able to propagate with supersonic speed and, therefore, is able to propagate upstream in a supersonic flow. As it propagates its amplitude shrinks and so eventually it comes to a halt at a position where its propagation speed, given by (2.34), exactly matches the one of the supersonic flow. In this way a steady-state shock front is formed. A real-world example of such a shock front is visible in the simulation results presented in Sect. 3.2.6, Fig. 3.25 as well as in the experimentally obtained interferometric image displayed in Sect. 4.4, Fig. 4.5.

As explained above, expansion shocks never occur because they violate the second principle law of thermodynamics and the expansion takes place as a continuous isentropic state change.

So far, the shock front has been considered a steady-state phenomenon but it is, of course, valid to use a coordinate system that is moving with velocity  $w_1$ , thus, co-moving with the flow prior to the shock. Then the shock front appears to propagate into the undisturbed medium with the velocity  $-w_1 = u$ . For the perfect gas with constant specific heat, this propagation speed of the shock front can be expressed by

$$u = c \sqrt{1 + \frac{\kappa + 1}{2\kappa} \frac{p_2 - p_1}{p_1}} \quad (2.34)$$

As mentioned above, this formula allows one to estimate the position of a steady state shock that forms in front of an obstacle in the flow.

A more realistic case for a propagating shock would be the one of a tube that is split into two parts by a wall confining a perfect gas of a certain pressure on one side and a perfect gas with lower pressure on the other. The sudden removal of the membrane results in a shock that travels into the lower pressure medium. But now, since no additional gas is added on the high pressure side, the pressure drops there as the shock propagates. This case can be treated within the more general framework of (supersonic) wave propagation in perfect gases. It is described in textbooks, for example [1] and gives the following result in the case of vacuum on the low pressure side of the membrane

$$w = \frac{2}{\kappa - 1} c_0 \quad (2.35)$$

Here,  $c_0$  is the sound velocity in the medium on the high pressure side prior to the removal of the wall and  $w$  is the velocity of the first disturbance that propagates into the vacuum. Given that the values of  $\kappa$  usually lie between 2.3 and 2.7, it is clear that this velocity can be significantly larger than the velocity of sound.

From the Eqs. 2.21–2.23 the following relations for the change of state in a shock front can be derived:

$$\frac{w_2}{w_1} = \frac{\rho_1}{\rho_2} = 1 - \frac{2}{\kappa + 1} \left( 1 - \frac{1}{M^2} \right) \quad (2.36)$$

$$\frac{p_2}{p_1} = 1 + \frac{2\kappa}{\kappa + 1} (M^2 - 1) \quad (2.37)$$

$$\frac{T_2}{T_1} = \frac{c_2^2}{c_1^2} = \frac{1}{M^2} \left[ 1 + \frac{2\kappa}{\kappa + 1} (M^2 - 1) \right] \left[ 1 + \frac{\kappa - 1}{\kappa + 1} (M^2 - 1) \right] \quad (2.38)$$

$$M_2^2 = \frac{1 + \frac{\kappa - 1}{\kappa + 1} (M^2 - 1)}{1 + \frac{2\kappa}{\kappa + 1} (M^2 - 1)} \quad (2.39)$$



$$\frac{s_2 - s_1}{c_v} = \ln \left[ 1 + \frac{2\kappa}{\kappa + 1}(M^2 - 1) \right] + \kappa \ln \left[ 1 - \frac{2}{\kappa + 1} \left( 1 - \frac{1}{M^2} \right) \right] \quad (2.40)$$

As can be seen, for the perfect gas with constant specific heat, the state change that occurs in a shock depends on the initial Mach number  $M = M_1$  only. Here,  $M$  is defined as  $M = w/c$  where  $w$  is the local velocity and  $c$  the local speed of sound according to Eq. 2.31. It must be kept in mind that these formulas are valid only for initial Mach numbers  $M \geq 1$  since for smaller Mach numbers isentropic expansion occurs. Figure 2.2 shows plots of the relations (2.36–2.40) for Nitrogen (solid black line), Argon (dashed black line), and Helium (solid red line). Since Argon and Helium are both monoatomic gases and, hence, have the same specific heat ratio of 5/3 and because only ratios are plotted the lines for these two gases coincide in all the plots. Again, it can be seen that the density ratio converges towards an asymptotic value while the pressure and temperature ratios grow without limits. Figure 2.2 shows the important fact that the flow is always subsonic after the shock with post-shock mach numbers decreasing as initial mach numbers increase. The entropy change normalized to the heat capacity  $(s_2 - s_1)/c_v$ , Fig. 2.2, can be used as a measure for the strength of the shock. To this end, however, it is also possible to define “local” reservoir conditions of a flow  $w_0 = 0, \rho_0, p_0, \dots$  as those conditions reached by bringing the flow isentropically to rest, thereby constituting the ideal conditions that could optimally be reached. Here, optimally means that in the case of isentropic compression, no pressure drop occurs and the initial reservoir conditions are obtained again. So, by definition, in an isentropic flow, the local reservoir conditions are constant throughout the flow. For the non-isentropic shock it follows from energy conservation that the local reservoir temperature is also constant but the local reservoir pressure and density drop with the amount of the drop being proportional to the strength of the shock.

$$\frac{\rho_{0,2}}{\rho_{0,1}} = \frac{p_{0,2}}{p_{0,1}} = \left[ 1 + \frac{2\kappa}{\kappa + 1}(M^2 - 1) \right]^{-\frac{1}{\kappa-1}} \left[ 1 - \frac{2}{\kappa + 1} \left( 1 - \frac{1}{M^2} \right) \right]^{-\frac{1}{\kappa-1}} \quad (2.41)$$

This equation is plotted in Fig. 2.2 showing that for low Mach numbers a shock is a quite efficient and for higher Mach numbers a quite inefficient way of decelerating and compressing a flow. Similar to the Eqs. 2.36–2.41, expressions for oblique shock fronts can be derived. The tangential velocity components are preserved by the shock for the shock-normal velocity components as well as for density, pressure, temperature, and local reservoir conditions, Eqs. 2.36–2.41 are still applicable by simply substituting  $M \sin \gamma$  for  $M$  where  $M = M_1$  is the Mach number before the shock and  $\gamma$  is the angle between the initial flow velocity and the shock front. Similarly to perpendicular shock fronts, the second principal law prohibits oblique expansion shocks as well. There are two extreme points for the pressure rise in the oblique shock, namely a maximum for  $\gamma = 90^\circ$  corresponding to a normal shock perpendicular to the flow and a minimum for  $\sin \gamma = 1/M = \sin \alpha$  with  $\alpha$  being the Mach angle. The latter represents the weakest possible distortion of a supersonic flow, so values of  $M \sin \gamma < 1$  are not meaningful.

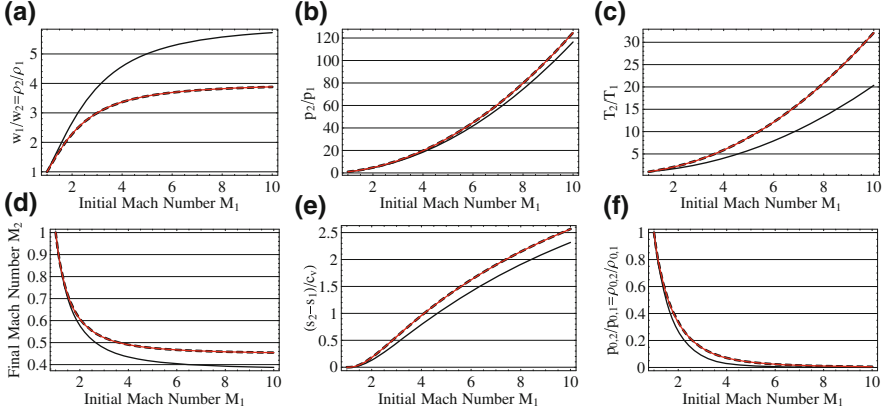


**Fig. 2.2** Change of important state variables in a normal shock in a perfect gas ( $N_2$ , solid black, Ar, dashed black, He, solid red line) with constant heat capacity. **a** Density. **b** Pressure. **c** Temperature. **d** Mach Number. **e** Entropy. **f** Local Reservoir Pressure

### 2.1.4 Continuous Flows in Nozzles

In the following, only continuous flows within nozzles are considered. Of course this does not mean that discontinuous shocks cannot occur within nozzles. It will briefly be discussed below under which conditions this will happen. However, for the case of interest here, namely a nozzle that is attached to a vacuum chamber, it is clear that no shocks can occur because expansion shocks are impossible. Therefore, in the following only the continuous case is treated extensively.

In order to describe flows that are bound and guided by walls within a 1-D theory it is necessary to introduce the cross section  $f$  of the gas-duct into the governing equations. This is most easily done regarding the differential equations corresponding to Eqs. 2.21–2.23 [1]:

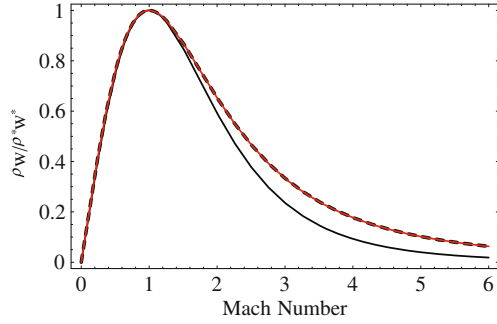
$$\frac{1}{w} \frac{dw}{dx} + \frac{1}{\rho} \frac{d\rho}{dx} + \frac{1}{f} \frac{df}{dx} = 0 \quad (2.42)$$

$$w \frac{dw}{dx} + \frac{1}{\rho} \frac{dp}{dx} = Y \quad (2.43)$$

$$w \frac{dw}{dx} + \frac{di}{dx} = \frac{dq}{dx} \quad (2.44)$$

Here (2.42) is the continuity equation, now including the flow cross section  $f$  ( $m^2$ ), (2.43) is the equation of motion including an external volume-force  $Y$  and (2.44) states energy conservation. In the case that there are no external forces and no energy or heat flows through the system boundaries,  $Y = 0$ ,  $dq/dx = 0$ , this corresponds to a continuous, isentropic flow  $ds/dx = 0$ . Then, by using (2.30) and  $M = w/c$  Eq. 2.43 can be written as

**Fig. 2.3** Flow density normalized to critical values in a converging–diverging flow for  $N_2$  black solid, Ar black dashed and He red solid



$$\frac{1}{\rho} \frac{d\rho}{dx} = -M^2 \frac{1}{w} \frac{dw}{dx} \quad (2.45)$$

This shows that for small Mach numbers the relative variation of the density is smaller than the relative variation of the velocity and for large Mach numbers vice versa. This leads to the limits of incompressible flow for very low Mach numbers, and, for high Mach numbers, to hypersonic flows where the maximum velocity (2.24) has (almost) been reached and stays more or less constant and only density, pressure, and temperature vary strongly.

By combining now Eqs. 2.45 and (2.42) the following relationship between the Mach number and the flow cross section can be derived:

$$(1 - M^2) \frac{1}{w} \frac{dw}{dx} = \frac{1}{\rho w} \frac{d(\rho w)}{dx} = -\frac{1}{f} \frac{df}{dx} \quad (2.46)$$

Here,  $\rho w$  is a new parameter called the flow density and gives the total mass flow after multiplication by the flow cross section,  $\dot{m} = \rho w f$ . The total mass flow, of course, has to be constant throughout the flow if no sources or sinks are present. Inspection of Eq. 2.46 shows that for subsonic flows the velocity grows with shrinking cross section and that for supersonic flows it grows with growing cross section. This effect is exploited in converging–diverging de Laval nozzles as depicted in Fig. 2.3. First in the converging section the flow accelerates up to  $M = 1$  which is reached in the throat. Then, in the diverging nozzle section, the flow is allowed to expand further thereby acquiring supersonic speeds corresponding to  $M > 1$ . For  $M = 1$  the flow cross section evidently has a minimum and the flow density a maximum and, therefore, this point in the flow is of special importance because it separates the sub- from the supersonic regime. The flow parameters that the gas obtains at that point are called “critical” parameters and are signed with an asterisk. These critical values can be calculated for the perfect gas with constant heat capacity as follows: Starting from Eq. 2.23, using (2.13) and assuming that the gas is initially at rest  $w_0 = 0$  one gets

$$\frac{w^2}{2} + c_p T = c_p T_0 \quad (2.47)$$

Here, variables with subscript 0 denote initial (reservoir) values. With (2.25) and (2.31) this transforms to

$$w^2 + \frac{2}{\kappa - 1}c^2 = w_{max}^2 \quad (2.48)$$

Here, the known critical values for  $M$  and  $w$ , namely  $M^* = 1$ ,  $w^* = c^*$  can be introduced leading to

$$w_{max}^2 = \frac{\kappa + 1}{\kappa - 1}(w^*)^2 = \frac{\kappa + 1}{\kappa - 1}(c^*)^2 = \frac{2}{\kappa - 1}c_0^2 = (\kappa + 1)c_p T^* = 2c_p T_0 \quad (2.49)$$

and, by exploiting the usual isentropic Eqs. 2.18–2.20, finally the following equations are obtained that now relate the relevant critical flow parameters to the reservoir values:

$$w^* = \sqrt{\frac{\kappa - 1}{\kappa + 1}2c_p T_0} = c_0 \sqrt{\frac{2}{\kappa + 1}} \quad (2.50)$$

$$\frac{p^*}{p_0} = \left(\frac{2}{\kappa + 1}\right)^{\frac{\kappa}{\kappa - 1}} \quad (2.51)$$

$$\frac{\rho^*}{\rho_0} = \left(\frac{2}{\kappa + 1}\right)^{\frac{1}{\kappa - 1}} \quad (2.52)$$

$$\frac{T^*}{T_0} = \frac{2}{\kappa + 1} \quad (2.53)$$

$$\frac{\rho^* w^*}{\rho_0 c_0} = \left(\frac{2}{\kappa + 1}\right)^{\frac{\kappa + 1}{2(\kappa - 1)}} \quad (2.54)$$

Now that the critical parameters are available, Eqs. 2.13, 2.18 and 2.22 can be used to calculate the flow density in the whole flow domain. Then, one arrives at the following result:

$$\frac{f^*}{f} = \frac{\rho w}{\rho^* w^*} = M \left[ 1 + \frac{\kappa - 1}{\kappa + 1}(M^2 - 1) \right]^{-\frac{\kappa + 1}{2(\kappa - 1)}} \quad (2.55)$$

A plot of this function is given in Fig. 2.3. Due to the continuity relation  $w\rho f = w^*\rho^*f^*$  the vertical axis in Fig. 2.3 can also be read as the cross section ratio  $f^*/f$  thereby showing that for each cross section two solutions are obtained, one corresponding to the subsonic and the other to the supersonic case. From  $M = 0$  to  $M = 1$  the flow accelerates towards the critical cross section and its flow density grows to its maximum value. As has been shown above, this requires a decreasing flow cross section that finally reaches a minimum value—the nozzle throat—where critical values are obtained. From there on, in order to further increase the Mach number, the flow cross section has to increase again in order to allow for the

additional expansion and the corresponding reduction of the flow density that is necessary to reach the supersonic regime. This converging–diverging nozzle is called a de Laval nozzle and is a very frequently used device for producing supersonic gas flows. The mass flow through the nozzle is now given by  $\dot{m}^* = \rho^* w^* f^*$  which evaluates to

$$\dot{m}^* = f^* \sqrt{\kappa \left( \frac{2}{\kappa + 1} \right)^{\frac{\kappa+1}{\kappa-1}} p_0 \rho_0} \quad (2.56)$$

while the mass flow in general is expressed by

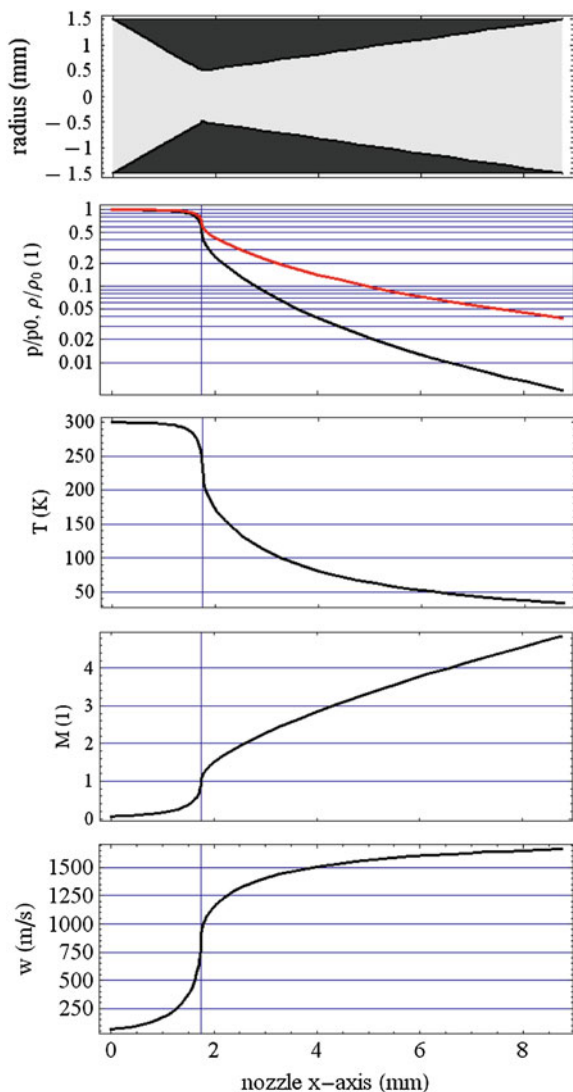
$$\dot{m} = f \sqrt{\frac{2\kappa}{\kappa - 1}} p_0 \rho_0 \left( \frac{p}{p_0} \right)^{\frac{1}{\kappa}} \sqrt{1 - \left( \frac{p}{p_0} \right)^{\frac{\kappa-1}{\kappa}}} \quad (2.57)$$

Since  $\dot{m}^* = \dot{m}$  holds everywhere in the flow domain, relation (2.57) implicitly defines the pressure  $p$  as a function of the cross section  $f$  in the whole flow. Comparable to Fig. 2.3, for the Mach Numbers—this equation has two solutions for  $p$  for each cross section  $f$ , one on the supersonic and one on the subsonic side of the critical cross section in the nozzle throat. With Eqs. 2.19, 2.20 the density  $\rho$  and the temperature  $T$  are calculated and the flow velocity  $w$  can be easily obtained via mass conservation from  $w = \dot{m}/(\rho f)$ .

Figure 2.4, shows plots of the most important flow parameters along a de Laval nozzle that is connected to a reservoir containing air at a pressure of 50 bar, a temperature of 300 K (corresponding to an initial density of  $1.2 \times 10^{21} \text{ cm}^{-3}$ ), and no initial velocity. The nozzle contour is also shown. It consists of a converging part with straight conical walls that is 1.75 mm long and has an entrance diameter of 3 mm. The throat diameter is 1 mm and subsequently the nozzle expands again with a straight conical contour to an exit diameter of 3 mm.

Tables 2.1 and 2.2 display numeric values of important flow parameters in the reservoir, at the throat where critical values are obtained and at the nozzle exit of a de Laval nozzle with a cross section ratio  $f_{\text{exit}}/f^*$  of 9. The pressure drops by almost a factor of 2 from the reservoir to the nozzle throat and subsequently in the supersonic section by a factor of 62. The density drop is less pronounced and reaches almost exactly a factor of 30 at the exit of the nozzle. The difference between the density and the pressure drop is explained by the fact that also the temperature decreases strongly—to 77 K at the nozzle exit—so that for the density that is a function of pressure and temperature some part of the pressure drop is compensated by the temperature drop. It is also interesting to note that the exit velocity of 670 m/s is already 86% of the theoretical maximum velocity (2.25) of 777 m/s. The mass flow through the nozzle amounts to 9.16 g/s which corresponds to a volume flux of 0.16 l/s at reservoir conditions (50 bar, 300 K). To give an impression of the influence of the type of gas used as a medium, in Table 2.2, the flow parameters for Helium are given using the same reservoir values. The medium enters the equations through two parameters, the molecular weight  $M$  and

**Fig. 2.4** Variation of flow parameters inside a de Laval nozzle with a cross section ratio  $f_{exit}/f^* = 9$ . Reservoir parameters:  $p_0 = 5 \times 10^6$  Pa = 50 bar,  $T_0 = 300$ K,  $w_0 = 0$ , medium: Helium. The parameters plotted are: nozzle radius *nozzle contour*, pressure *black*, and density *red* normalized to their respective reservoir values, temperature (K), Mach number (1) and flow velocity (m/s)



the heat capacity (for constant pressure)  $c_p$ . For air, the average molecular weight is 28.9696 g/mol and  $c_p$  is 1006.43 J/kg K, helium has a molecular weight of 4.0026 g/mol and a  $c_p$  of 5193 J/kg K. Inspection of the equations show, however, that in almost all the cases the parameter  $\kappa$ —which is a function of both  $c_p$  and  $M$ —is the only medium-dependent parameter. As mentioned above, the significance of  $\kappa$  lies in the fact that  $2/(\kappa - 1)$  corresponds to the number of degrees of freedom of the gas molecules. Its value is 2.4 for Air and 2.67 for helium which corresponds to 5 degrees of freedom for the *average* air molecule and 3 degrees of freedom—only the translations—for the point-like helium atom. The main

**Table 2.1** Flow variables in a de Laval nozzle

Parameter	Reservoir	Throat	Nozzle exit
Pressure (bar)	50	26.4	0.429
Density ( $10^{19} \text{ cm}^{-3}$ )	121	76.5	4.02
Temperature (K)	300	250	77.2
Mach Number (1)	0	1	3.80
Velocity (m/s)	0	317	670

Medium: air. Entrance diameter 3 mm, throat diameter 1 mm. Exit diameter 3 mm. Reservoir parameters:  $p_0 = 5 \times 10^6 \text{ Pa} = 50 \text{ bar}$ ,  $T_0 = 300 \text{ K}$ ,  $w_0 = 0 \text{ m/s}$

**Table 2.2** Flow variables in a de Laval nozzle

Parameter	Reservoir	Throat	Nozzle exit
Pressure (bar)	50	24.4	0.218
Density ( $10^{19} \text{ cm}^{-3}$ )	121	78.4	4.627
Temperature (K)	300	225	34.1
Mach Number (1)	0	1	4.84
Velocity (m/s)	0	882.6	1662

Medium: helium. Entrance diameter 3 mm, throat diameter 1 mm. Exit diameter 3 mm. Reservoir parameters:  $p_0 = 5 \times 10^6 \text{ Pa} = 50 \text{ bar}$ ,  $T_0 = 300 \text{ K}$ ,  $w_0 = 0 \text{ m/s}$

differences between the air flow and the helium flow are the following: the smaller molecular weight of He manifests itself in a much higher exit velocity of 1,662 m/s which compares to a theoretical maximum velocity of 1,765 m/s. The smaller heat capacity leads to a much smaller exit temperature of 34.1 K as compared to 77.2 K for air which also leads to a higher Mach number for helium of 4.84. The density at the exit is almost the same, the pressures differ by a factor of 2. The mass flow is smaller by a factor of 2.5 for Helium but the volume flow is higher by a factor of 2.8—another effect of the small molecular weight of helium. If the jet is assumed to emanate into vacuum it is not possible within this simple model to predict its evolution outside the nozzle because the flow cross section is not a priori known and cannot easily be calculated. Also, within the nozzle the presented model is accurate only as long as the part of the flow that is affected by the presence of walls is negligibly small in comparison to the flow dimensions. Since the processes within the wall-affected zone, the so-called boundary layer, depend non-trivially on flow parameters like pressure, pressure gradient, velocity, fluid viscosity, and turbulence, there are no sufficiently accurate analytical models that would allow to study this phenomenon in analytical fashion. Therefore, one has to rely on numeric simulation of the flow which will be the central point of the following chapter.

To conclude this section, Fig. 2.5, gives an overview over the dependence of important state variables at the exit of the de Laval nozzle on backing pressure, cross section ratio between nozzle throat and exit, reservoir temperature, and on the gas type. In all the plots, the plot for Helium is the solid red, the one for Argon the dashed black, and the one for  $N_2$  the solid black line. Since Argon and Helium are both monoatomic gases with the same isentropic exponent it is expected that

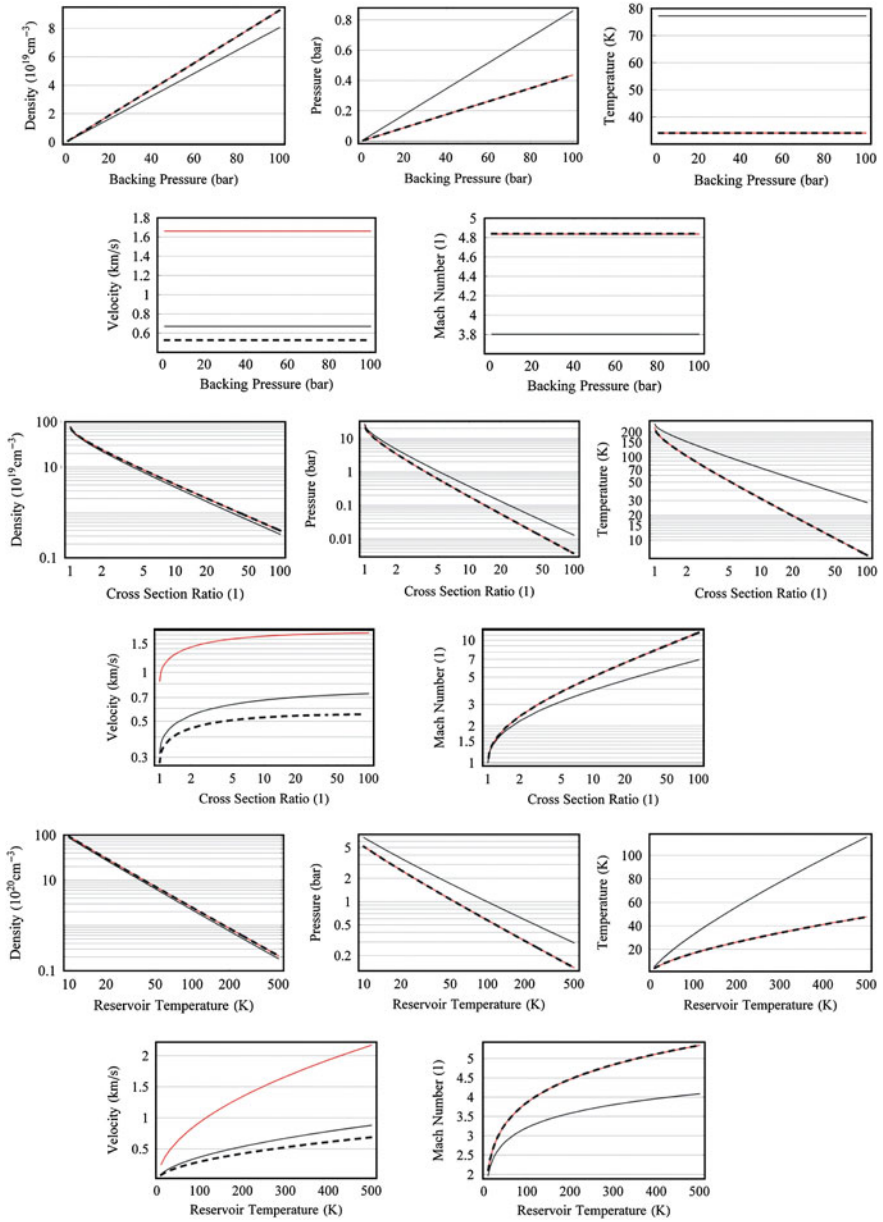


**Fig. 2.5** Variation of relevant state variables with backing pressure *upper five plots*, ratio between exit and throat cross sections *middle five plots*, and reservoir temperature *lower five plots*. Medium: Helium *solid red*, Argon *dashed black*,  $N_2$  *black*



they show similar behavior. For the upper five and the lower five plots, a cross section ratio of nine was used, for the middle five plots the backing pressure was set to 50 bar. Looking first at the upper five plots in the figure it can be seen that the (particle) density and pressure vary linearly with backing pressure. Since density is measured in particles per  $\text{cm}^3$  and not in  $\text{kg}/\text{m}^3$ , the two lines for Argon and Helium overlap showing exactly the same result. The (static) pressure at the nozzle exit also depends linearly on the backing pressure and, again, Argon and Helium give the same results. Temperature, velocity, and Mach number do not depend on the backing pressure at all. It is apparent that the exit velocity is the only parameter that actually depends on the molecular weight of the gas showing different results for Argon and Helium.

Turning now to the middle five plots, it is clear that by changing the cross section ratio between the nozzle exit and throat, the flow parameters at the nozzle exit readily vary over orders of magnitude, therefore, all plots are in double logarithmic scale. Again, the exit velocity is the only parameter where Argon and Helium show different results. The almost linear behavior of density, pressure, and temperature at the nozzle exit imply a power law dependence on the cross section ratio. The exit velocity rapidly converges to the maximum attainable speed which is given by energy conservation (see 2.25). The fact that the Mach number keeps growing is explained by the falling temperature that lowers the speed of sound.

The lower five plots show the dependence of the flow conditions at the nozzle exit on the temperature of the gas reservoir. Particle density and pressure follow almost perfectly a power law (double logarithmic plots). Interestingly, the exit temperature varies rather gently with the initial temperature. Since it can be seen that velocity and, therefore, also the Mach number vary with the reservoir temperature, it represents a convenient way of tuning the velocity and Mach number at the nozzle exit. Especially the latter one can be of importance because in the case that supersonic shock fronts are used in the experiment, the ratio of all the flow parameters before and after the shock only depend on the Mach number (see Eqs. 2.36–2.40).

### ***2.1.5 Cluster Formation in Supersonic Gas Jets***

It is a long known fact that high pressure gas jets emanating into vacuum can be a formidable way of producing large clusters of atoms or molecules [2–6]. This is due to the high densities and low temperatures that are simultaneously reached in such jets. Since de Laval nozzles are especially well suited for reaching both—high density and low pressure—at the nozzle exit, they are especially effective tools for cluster formation. Since the presence of clusters in a gas jet may have an influence on any experiments conducted with these jets, a short analysis of the cluster production in supersonic gas jets is presented.

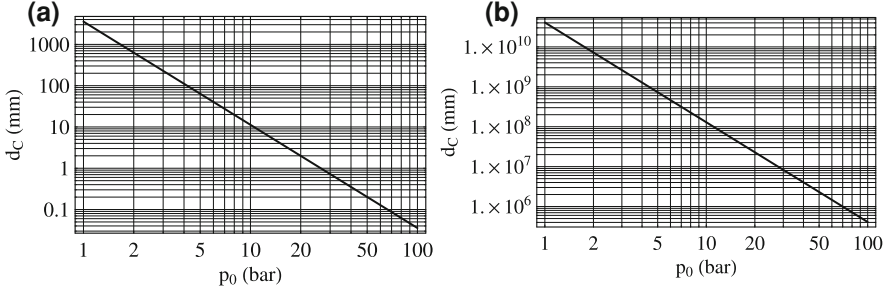


**Fig. 2.6** Plots of critical nozzle diameters and backing pressures that lead to a dimer mole fraction of 0.01 which is considered as the onset of clustering. **a** Argon. **b** Helium

Since dimers are the first step in cluster formation, the dimer mole fraction  $X_{A_2}$  represents a meaningful measure for the number of clusters to be expected in a gas jet. The dimer formation goes on continuously from the nozzle throat diameter downstream until the so-called sudden freeze surface is reached beyond which no more significant condensation into clusters occurs any more [3]. The position of this surface is essentially a function of temperature and can be assumed to lie several nozzle diameters away from the nozzle exit in the case of small diameter ratios ( $<4:1$ ) of the de Laval nozzle. Therefore, the final dimer mole fraction can be regarded an upper limit of the dimer content close to the nozzle exit. In order to calculate the final dimer mole fraction the following empirical formula is given in [3]:

$$X_{A_2} = \frac{1}{2} \left( \rho_p \sigma^3 \left( \frac{\varepsilon}{k_B T} \right)^{\frac{7}{5}} \left( \frac{d^*}{\sigma} \right)^{\frac{2}{5}} \right)^{\frac{5}{3}} \quad (2.58)$$

Here,  $\rho_p$  is the gas number density,  $\sigma$  is the atom size,  $\varepsilon$  is the potential well depth,  $k_B$  is Boltzman's constant,  $d^*$  is the critical (smallest) diameter of the nozzle. Values for these parameters can be found in [3] and [7]. For Helium the following values are used:  $\sigma = 2.66 \times 10^{-10} \text{m}$ ,  $\varepsilon/k_B = 10.9 \text{K}$ , and for Argon  $\sigma = 3.33 \times 10^{-10} \text{m}$ ,  $\varepsilon/k_B = 144.4 \text{K}$ . In the case of a de Laval nozzle for  $d^*$  the following expression is substituted [3], [4]:

$$d_{eq}^* = 0.736 d_C \cot(\alpha), \quad \gamma = 5/3 \quad (2.59)$$

$$d_{eq}^* = 0.866 d_C \cot(\alpha), \quad \gamma = 7/3 \quad (2.60)$$

where  $d_{eq}^*$  is an equivalent diameter that depends on the gas type defined by the specific heat ratio  $\gamma$ , the half opening angle  $\alpha$ , and the throat diameter  $d_C$ . According to [2, 3, 8], considerable clustering sets in for mole fractions larger than 0.01. This is shown in Fig. 2.6, where those value pairs of  $d_C$  and  $p_0$  are plotted that correspond to a value of  $X_{A_2}$  of 0.01. In order to have no clusters, parameters below the lines have to be chosen. As can be seen, this is posing some limits on

pressure and/or nozzle diameter for Argon whereas for Helium no clusters can be expected in a realistic pressure and diameter range. For de Laval nozzles, the expressions given by Eqs. 2.59 and 2.60 must be substituted for  $d_C$ .

## References

1. Oswatitsch, K.: *Gasdynamik*. Springer, Heidelberg (1952)
2. Knuth, E.L.: Size correlations for condensation clusters produced in free-jet expansions. *J. Chem. Phys.* **107**(21), 9125–9132 (1997)
3. Knuth, E.: Dimer-formation rate coefficients from measurements of terminal dimer concentrations in free-jet expansions. *J. Chem. Phys.* **66**(8), 3515–3525 (1977)
4. Hagena, O.F.: Nucleation and growth of clusters in expanding nozzle flows. *Surf. Sci.* **106**, 101 (1981)
5. Bauer, S.H., Chiu, N-S., Wilcox, C.F. Jr.: Kinetics of condensation in supersonic expansion (ar). *J. Chem. Phys.* **85**(4), 2029–2037 (1986)
6. Hillenkamp, M., Keinan, S., Even, U.: Condensation limited cooling in supersonic expansions. *J. Chem. Phys.* **118**(19), 8699–8705 (2003)
7. Hirschfelder, J.O., Curtiss, C.F., Bird, R.B.: Wiley, (1964)
8. Scheier, P., Märk, T.D.: Isotope enrichment in ne clusters. *J. Chem. Phys.*, **87**(9), 5238–5241 (1987)

<http://www.springer.com/978-3-642-19949-3>

Laser Wakefield Electron Acceleration  
A Novel Approach Employing Supersonic Microjets and  
Few-Cycle Laser Pulses

Schmid, K.

2011, XIV, 166 p., Hardcover

ISBN: 978-3-642-19949-3